

A Cracked Pipe Element Coupling Plasticity and Crack Growth for Leak before Break Applications

J. BROCHARD, A. COMBESURE, PH. JAMET
CEA-CEN Saclay, Gif sur Yvette, France

1 INTRODUCTION

The so-called "cracked pipe element" is a finite element, which is applicable for fracture assessment of piping systems, with postulated circumferential through-wall cracks in the straight parts. Considered loads are an axial force and an in-plane bending moment. Those loads may be static or dynamic.

The objectives carried on, for this element, are:

- a good representation of the flexibility of a cracked pipe,
- a good prediction of the limit loads,
- an efficient tool for fracture assessment: determination of the stress intensity factor, the crack area, J - value and crack growth.

This element has been implemented in the finite element computer code CASTEM 2000. The elastic and plastic properties of the model were earlier presented (Brochard et al., 1989).

In this paper, we present:

- for the elastic plastic behaviour, a new engineering method, based on experimental data, to predict the moment-rotation relation,
- the iterative algorithm used for crack growth.

Application on tests of the Degraded Piping Program is then discussed.

2 FORMULATION OF THE PLASTICITY FOR THE CRACKED PIPE ELEMENT

Formulation of the plasticity for the cracked pipe element is based on the following assumptions:

- all plastic deformations of the simulated straight pipe are affected to the cracked pipe element,
- the stress field in the cracked section is governed by a limit-stress diagram (fig. 1).

Integrating the limit-stress diagram, we obtain the expression of the axial force and the bending moment as functions of the geometrical parameters, the reference stress σ_0 and the neutral axis position α_0 :

$$M = \int_{-\pi/2}^{\pi/2-\theta} \sigma z \, ds = 2 \sigma_0 R^2 t (2 \cos \alpha_0 - \sin \theta)$$

$$N = \int_{-\pi/2}^{\pi/2-\theta} \sigma \, ds = 2 \sigma_0 R t (2 \alpha_0 - \theta)$$

with R: radius; t: thickness; θ : half crack angle.

Eliminating α_0 , we deduce the equation of the plastic loading surface:

SMIRT 11 Transactions Vol. G (August 1991) Tokyo, Japan, © 1991

$$F_1 (M, N, \theta, \sigma_o) = \frac{M}{M_o} - \cos \frac{1}{2} \left(\theta + \pi \frac{N}{N_o} \right) + \frac{1}{2} \sin \theta$$

$$\text{with } M_o = 4 \sigma_o R^2 t \quad \text{and} \quad N_o = 2 \sigma_o \pi R t$$

In order to be applicable in case of dynamic loadings, the loading surface must be completed by the surface corresponding to the closing mode:

$$F_2 (M, N, \theta, \sigma_o) = - \frac{M}{M_o} - \cos \frac{1}{2} \left(\theta - \pi \frac{P}{P_o} \right) + \frac{1}{2} \sin \theta$$

The loading surfaces for different σ_o levels are plotted in fig. 2.

Supposing a given moment-rotation relation $M = f(\phi)$, characterizing the cracked pipe elastic plastic behaviour, plastic flow is determined by means of an iterative algorithm to solve:

$$F(M, N, \theta, \sigma_o) = 0 \quad (F = F_1 \text{ or } F_2)$$

$$\text{with } \begin{cases} M = f(\phi) & \text{moment-rotation curve} & M = 4 \sigma_o R^2 t \left(\cos \frac{\theta}{2} - \frac{1}{2} \sin \theta \right) \\ \phi = \phi_e + \phi_p & \phi_e = c_M M \end{cases}$$

3 EVALUATION OF THE MOMENT-ROTATION RELATION

3.1 Brief review of approximale methods

To evaluate the moment-rotation relation, different authors proposed approximate methods. We briefly review two of them:

- Tada's and Paris's procedure (1983) interpolates between the elastic and fully plastic solution by means of a "plastic zone size correction".
- LBB.NRC method (Klecker et al., 1986) is based also on the Irwin correction, but with an additional plastic component of the rotation, related to the applied stress level by the Ramberg-Osgood parameters.

Another procedures have been recently developped (Brust, 1987).

3.2 The DEFR method

As an alternative to these engineering methods based on analytical considerations, we developped another method based on experimental data.

Principle of this method is to establish relations between the plastic component of the rotation and an equivalent strain, we call reference strain, connected to the reference stress by the material stress-strain curve. To reach this goal, we use results of four-point bending experiments carried out by CEA on 4 inch diameter tubes (Moulin et al., 1989) (fig. 3). Tubes with circumferential through-wall crack ranging from 15 to 150 degrees were tested. Material was 316L stainless steel. Two types of notches were machined in the test pipes (fig. 4). Smooth defects didn't propage during test, whereas fatigue pre-cracked defects grew on a few millimeters. Considering the fact that we wanted to represent just the elastic plastic behaviour, without taking into account fracture mecanism, we had to analyse only tests conducted on smooth defects. Rotations near and far from the crack plane were measured (fig. 5), and records were put in a suitable form for our analysis. The recorded moment-rotation curves for smooth defects are plotted in fig. 6. In the same time, tensile tests were conducted in specimens machined from the tubes. From all these records, we elaborated a dimensionless diagram $(\epsilon_p/\epsilon_e, \phi_p/\phi_e)$, for each crack size, using the following procedure for different moment levels:

- determine the reference stress:

$$\sigma_o = \frac{M}{4 R^2 t A(\theta)} \quad \text{with} \quad A(\theta) = \cos \frac{1}{2} \theta - \frac{1}{2} \sin \theta$$

- transfer the σ_o value on the material stress-strain curve normalized by σ_F , to obtain the elastic and plastic components of the reference strain: ϵ_e, ϵ_p ,
- transfer the M value on the (M, ϕ) curve to obtain the elastic and plastic components of the rotation: ϕ_e, ϕ_p .

The so-determined ($\epsilon_p/\epsilon_e, \phi_p/\phi_e$) diagrams depend on the crack size (fig. 7). It was included in computer code CASTEM 2000, to be used as an experimental data basis for prediction the moment-rotation relation of any cracked pipe, from its material stress-strain curve.

4 COUPLING BETWEEN PLASTICITY AND CRACK GROWTH

To solve plasticity and crack growth coupling, one has to solve together the following equations:

$$\begin{cases} F(M, N, \sigma_o, \theta) = 0 & (1) \\ J_e(\theta) + J_p(\theta) - J_m(\theta) = 0 & (2) \end{cases}$$

where the elastic and plastic components of the J-parameter are calculated by the following expressions:

$$J_e = K_f M \quad \text{with} \quad K_f = \frac{\sqrt{\pi R \theta}}{\pi R^2 t} F_f(\theta/\pi)$$

$$J_p = \int_0^{\phi} \frac{M}{4 R^2 t A(\theta)} R \left(\cos \theta + \frac{1}{2} \sin \theta \right) d\phi_p$$

and J_m designs the value of J on the resistance curve for the crack growth $\Delta\theta = \theta - \theta_o$ (θ_o being the initial crack angle).

To simplify this a bit tricky problem, we enter as data of the nonlinear computations using the cracked pipe element, a moment-rotation relation that verifies equation (2), that means a (M, ϕ) relation with crack growth effects included. Then the problem is solved using the same algorithm described in § 2, which is proved to be applicable in case of non monotonic (M, ϕ) curve.

From the (J, Δa) resistance curve and the (M, ϕ) relation, characterizing the elastic plastic behaviour of the cracked pipe (obtained either with the DEFR method or another method), the (M, ϕ) relation with crack growth effects included is determined by means of an iterative algorithm. The iterative method interpolates into a system of (M, ϕ) curves, with increasing crack angles, in order to determine, for a given rotation value ϕ , the crack angle θ for which equation (2) is verified (fig. 8).

5 APPLICATION ON EXPERIMENTS OF THE DEGRADED PIPING PROGRAM

We present here application of the DEFR method and other approximate methods for prediction of the moment-rotation relation in case of three experiments of the Degraded Piping Program (Wilkowski, 1984-1989). Several analyses were presented earlier by Brust (1989), by means of comparisons of load versus load-line displacement records. The load-line displacement is the sum of three contributions:

- compliance of the machine,
- bending of the straight part,
- additional displacement due to the crack.

In order to clearly show up discrepancies, if there are, between additional displacement due to the crack predicted by the engineering methods, and evaluated from experimental data, we converted the load versus load-line displacement data into moment versus crack rotation data.

Experiments numbered 4111-3, 4141-1 and DTPIPE 7 were analysed. Pipe identifications for material characterization are respectively DP2-A12-1 and DP2-A12-5 (J_M curve) for 4111-3 test, DP2-A23-1 and DP2-A45W-2 (J_D curve) for 4141-1 test. For DTPIPE 7 test, we took into account material properties used by Brust (1989). For these three pipes, crack angles ranged from 110.6 to 133.56 degrees.

Experiment 4111-3 was conducted on a 42-inch nominal diameter stainless steel pipe. For this large pipe, J-R curves from small specimens are too limited to predict the large amounts of crack growth recorded during the test. As we did not extrapolate the J-R curve, our predicted moment-rotation curves are limited to small rotations (fig. 9).

Experiment 4141-1 was conducted on 6-inch nominal diameter stainless steel pipe. The crack was machined in the centerline of a submerged-arc weld. For this test, there is a strong difference between predicted and measured elastic stiffnesses. This discrepancy was found earlier in Brust's analysis, but majored in our analysis, in which just the crack contribution is considered. However, we can note that the DEFR method predicts the largest plastic rotations (fig. 10).

Experiment DTPIPE-7 was conducted on a 8-inch nominal diameter carbon-steel pipe. For this test, the different methods give quite accurate predictions (fig. 11).

6 CONCLUSION

In its actual version, the cracked pipe element is proved to be an efficient tool for Leak Before Break assessment of cracked piping system, subjected to static or dynamic loads. (Petit et al., 1989).

But the precision of results obtained using this finite element depends on the accuracy of the moment-rotation data. The accuracy of (M, ϕ) relation could be affected by a bad prediction of the additional plastic flexibility due to the crack and also by a bad extrapolation of the CT specimen resistance curve. For plastic flexibility prediction, a new engineering method, based on experimental data, has been developed. First applications on DPIP experiments are encouraging.

REFERENCES

- Brochard, J., Petit, M. Millard, A. (1989). A special cracked pipe element for Leak Before Break applications, Transactions of the 10th SMIRT, Vol. G, pp 357-362.
- Paris, P.C. and Tada, H. (1983). The application of fracture proof design methods using tearing instability theory to nuclear piping postulating circumferential through-wall cracks, NUREG/CR-3464.
- Klecker, R., Brust, F. and Wilkowski, G. (1986). NRC Leak-Before-Break (LBB.NRC) analysis method for circumferentially through-wall cracked pipes under axial plus bending loads, NUREG/CR-4572.
- Brust, F.W. (1987). Approximate methods for fracture analyses of through-wall cracked pipes, NUREG/CR-4853.

Moulin, D. et al. (1989). Experimental evaluation of J in cracked straight and curved pipes under bending, Transactions of the 10th SMIRT, Vol. G, pp 323-326.

Wilkowski, G.M., et al. (March 1984 - January 1989) Degraded Piping Program Phase II, NUREG/CR-4082.

Petit, M. and Jamet, Ph. (1989). Numerical evaluation of cracked pipes under dynamic loading using a special finite element, Transactions of the 10th SMIRT, Vol. G, pp 341-346.

Jamet, Ph, Faigy, C. and Bhandari, S. (1991). French piping integrity research program for PWR, to be published in the transactions of the 11th SMIRT.

ACKNOWLEDGMENT

This work was done as part of the french piping integrity research program for PWR (Jamet et al., 1991), and also with the financial support of the safety authorities of C.E.A.

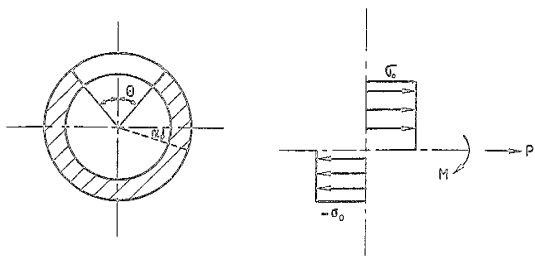


Fig. 1 - Limit - stress diagram

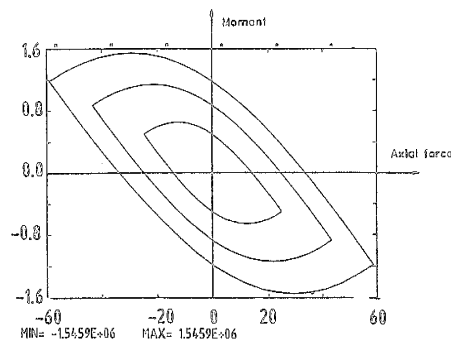


Fig. 2 - Plastic loading surfaces

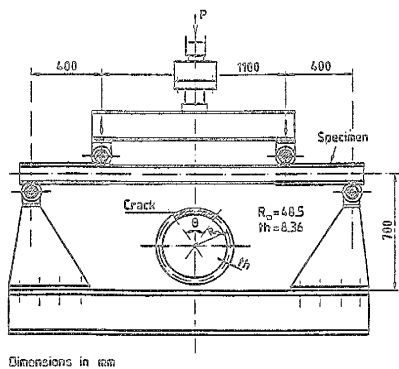


Fig. 3 - Experimental device for four-point bending tests

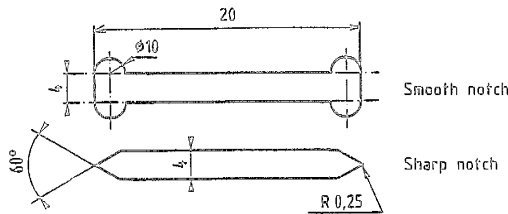


Fig. 4 - Notch geometries

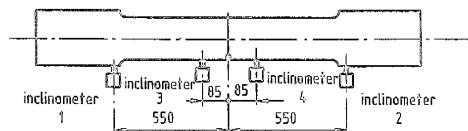


Fig. 5 - Inclometers for rotation records

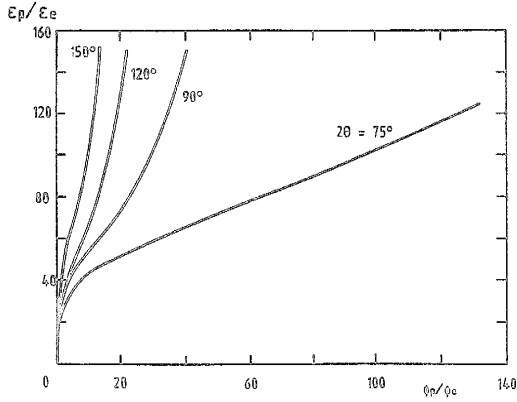


Fig. 7 - $(\epsilon_p/\epsilon_e, \phi_p/\phi_e)$ diagrams

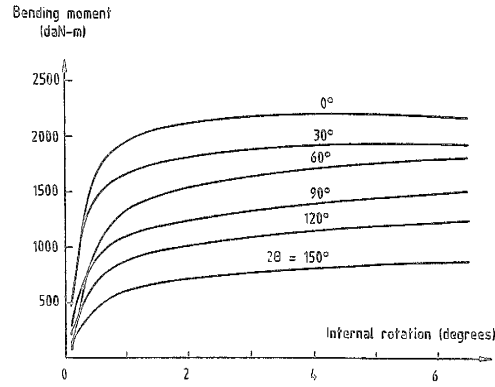


Fig. 6 - Moment - internal rotation curves

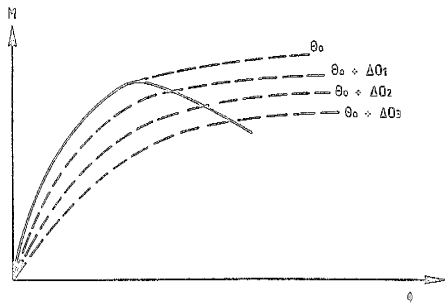


Fig. 8 - Interpolation in (M, ϕ) curve system

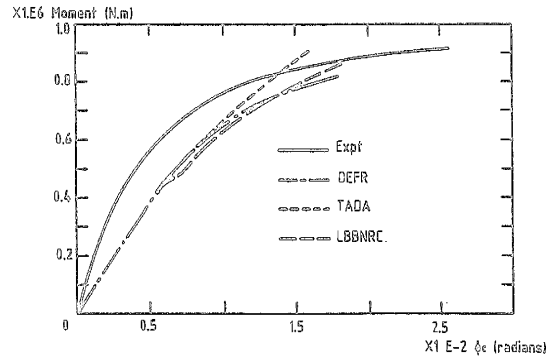


Fig. 9 - Moment - rotation predictions for experiment 411-3

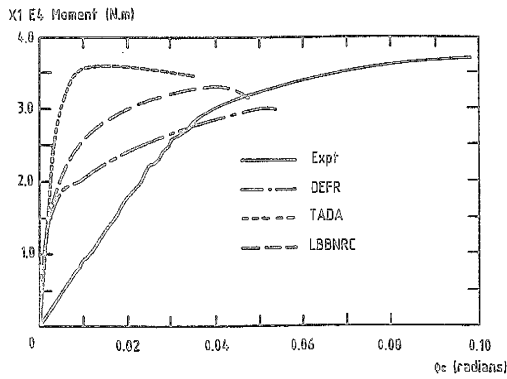


Fig. 10 - Moment - rotation predictions for experiment 414-1

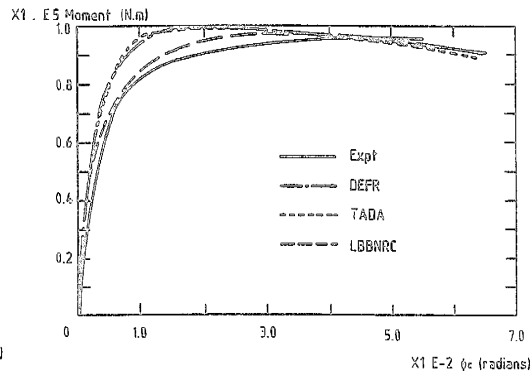


Fig. 11 - Moment - rotation predictions for experiment DTPPE 7